Buckled Plate Vibrations and Large Amplitude Vibrations Using High-Order Triangular Elements

T. Y. Yang* and A. D. Han†
Purdue University, West Lafayette, Indiana

A high-order triangular membrane finite element is combined with a fully conforming triangular plate bending element to solve the geometrically nonlinear problems of plates where the membrane and flexural behaviors are coupled and the effect of the inplane boundary conditions is as significant as the flexural boundary conditions. Each of the three orthogonal displacement components is represented by a two-dimensional polynomial of the same quintic order with no bias against one another giving the element a total of 54 degrees of freedom. The nonlinear stiffness matrices are formulated and a Newton-Raphson iteration procedure is used. Examples include the analyses of plane stresses of a parabolically loaded square plate, large deflections of a square plate under lateral pressure, postbuckling of a square plate, linear free vibration of a buckled rectangular plate, large amplitude free vibration of a square plate with and without inplane stresses. Various flexural and inplane boundary conditions are considered. Results are compared with those obtained by alternative finite element methods, analytical approximate methods, and an experiment. Physical interpretations of the results and explanations of the discrepancies among various solutions are provided. The results indicate that the present development is capable of accurately solving a wide variety of geometrically nonlinear plate problems.

Introduction

THE early and fundamental works on the problem of static bending of plates with large deflections are well documented.[1] Way[2] used the Ritz energy method with polynomials satisfying the boundary conditions. Levy[3,4] employed the trigonometric series to solve the von Kármán equations. Wang[5] used the finite difference technique to solve the governing equations. Berger[6] proposed an approximate approach which simplified the nonlinear equations by neglecting the second invariant of the membrane strains.

The problem of postbuckling of rectangular plates under edge compression was well investigated. The early works using approximate solutions for simply supported plates were reviewed by Coan.[7] Solutions of a theoretically exact nature using trigonometric series were done by Levy[3] and Coan.[7] Yamaki[8] extended Levy and Coan's works for various boundary conditions.

The problem of small amplitude vibration of a buckled rectangular plate with aspect ratio of 3 was studied by Bisplinghoff and Pian.[9] Equations of motion were derived from Lagrange's equation for the total potential energy of the plate subjected to inplane loading. Results for nondimensional frequency vs inplane loading were obtained for the symmetrical modes both analytically and experimentally.

The problem of large amplitude vibrations of plates was studied extensively. Herrmann[10] proposed a nonlinear plate theory of motion corresponding to the dynamic analog of von Kármán's theory. Chu and Herrmann[11] used the perturbation method to study a simply supported rectangular plate with four edges fixed from inplane movement. Yamaki[12] used Galerkin's method with one-term approximation to study both the simply supported and clamped plates with three different cases of inplane boundary conditions. Wah[13] extended Berger's approximate method[6] to solve the vibration problem. A survey of the studies on large amplitude vibration of plates covering the period from 1961 to 1973 was given by Pandalai.[14]

The problem of nonlinear vibration of plates under initial stresses was studied by Eisley.[15] Galerkin's method with one-term representation was used. Both the simply supported and the clamped beams and plates were considered. The results for the postbuckling region were included.

An alternative approach to solve these static and dynamic geometrically nonlinear problems of plates is to use the finite element method. A review of the early developments of the finite element method to solve the static and postbuckling problems of plates with large deflections can be found, for example, in Ref. 16.

The use of the finite element equations to solve the nonlinear dynamic problems was investigated by McNamara and Marcal.[17] Application of the finite element method to solve the large amplitude vibration problem of plates was reported by Mei.[18] He assumed constant stresses within each element. Rao et al.[19] presented a linearized strain-displacement relation for a plate with immovable edges. Mei et al.[20] used the 18 degree-of-freedom (d.o.f.) triangular plate element by Cowper et al.[21] to investigate the large amplitude vibrations of plates of arbitrary shapes. Mei[22] also used the 16 d.o.f. rectangular plate element to study large amplitude vibrations of plates with initial stresses. In Refs. 19, 20, and 22, the inplane strains $\partial u/\partial x$, $\partial v/\partial y$, $\partial u/\partial y$, and $\partial v/\partial x$ were neglected and, thus, no inplane degrees of freedom were assumed in their element formulations. In all of their examples, edges were fixed from inplane movements.

When reviewing the preceding developments of the finite element method, a general deficiency is seen. The existing element formulations lack the ability to accurately account for the effect of inplane displacements and, consequently, the complex inplane boundary conditions. A majority of the publications assumed that the edges were immovable in the middle plane. The other two common and physically possible boundary conditions such as keeping the edges straight and freeing the edge stresses were neglected. Such deficiency is particularly critical and evident in the finite element solutions for plates in postbuckling.[16,23] A cause of such deficiency appears to be in the previous investigators' assumption that the inplane polynomial displacement functions are of lower order than the transverse deflection function for the plate element.[16,23]

During such review, it is also found that some cases of practical significance have not been studied using finite elements, such as linear vibration of buckled plates and large amplitude vibration of plates with movable edges.

Recently, Tabarrok and Dost[24] proposed four variational formulations for large deformation analysis of thin elastic

Received April 8, 1982; revision received July 19, 1982.

*Professor and Head, School of Aeronautics and Astronautics. Associate Fellow AIAA.

†Graduate Student, School of Aeronautics and Astronautics.

plates. The von Kármán equations were cast into the mixed finite element formulations.[25] In von Kármán's formulation, the total potential energy involves quadratic and cubic terms of the derivatives of displacements and stress functions, whereas in the common displacement formulation, it contains terms of displacement derivatives up to the quartic power.

In this study, the scope is limited to the finite element displacement model. The 54 d.o.f. triangular element developed by Dawe[26] for small deflection analysis of shells is used. Each node has six d.o.f.'s for each of the three displacements (u, v, and w) including up to second-order derivatives of each displacement with respect to the coordinates x and y. All three displacement functions are of the same quintic order.

Performance of this element in predicting the inplane behavior is evaluated by comparing the results with an alternative finite element solution[27] for a parabolically loaded plane stress problem and excellent accuracy and efficiency are found. Incremental stiffness matrices are derived based on three equally competent quintic displacement functions. The ability gained in more accurately accounting for the effect of inplane displacements enables this study to tackle a wide variety of plate problems with arbitrary inplane boundary conditions. The cases considered include bending of plates with large deflections, postbuckling of plates, small amplitude vibration of a buckled plate, large amplitude vibration of plates with and without inplane forces; all with three basic inplane boundary conditions: edges fixed, edges kept straight, and edges stress free. All the results are evaluated by comparison with alternative analytical, Galerkin, finite element, and experimental solutions. Discussions are given.

Strain Energy for Plates with Large Deflection

From von Kármán's large deflection theory of plates, the strain-displacement relations are defined as

$$\epsilon_x = \frac{\partial u}{\partial x} + \frac{1}{2}\left(\frac{\partial w}{\partial x}\right)^2 - z\frac{\partial^2 w}{\partial x^2} \tag{1}$$

$$\epsilon_y = \frac{\partial v}{\partial y} + \frac{1}{2}\left(\frac{\partial w}{\partial y}\right)^2 - z\frac{\partial^2 w}{\partial y^2} \tag{2}$$

$$\epsilon_{xy} = \frac{\partial u}{\partial y} + \frac{\partial v}{\partial x} + \left(\frac{\partial w}{\partial x}\right)\left(\frac{\partial w}{\partial y}\right) - 2z\frac{\partial^2 w}{\partial x \partial y} \tag{3}$$

where u, v, and w are the three displacement components in x, y, and z directions, respectively. Based on Eqs. (1-3), the strain energy expression for a plate can be obtained as

$$U = U_1 + U_2 + U_3 + U_4 \tag{4}$$

with

$$U_1 = \frac{6D}{h^2}\iint\left\{\left(\frac{\partial u}{\partial x}\right)^2 + 2\nu\left(\frac{\partial u}{\partial x}\right)\left(\frac{\partial v}{\partial y}\right) + \left(\frac{\partial v}{\partial y}\right)^2 + \frac{1-\nu}{2}\left(\frac{\partial u}{\partial y} + \frac{\partial v}{\partial x}\right)^2\right\}dxdy \tag{5}$$

$$U_2 = \frac{D}{2}\iint\left\{\left(\frac{\partial^2 w}{\partial x^2}\right)^2 + 2\nu\frac{\partial^2 w}{\partial x^2}\frac{\partial^2 w}{\partial y^2} + \left(\frac{\partial^2 w}{\partial y^2}\right)^2 + 2(1-\nu)\left(\frac{\partial^2 w}{\partial x \partial y}\right)^2\right\}dxdy \tag{6}$$

$$U_3 = \frac{6D}{h^2}\iint\left\{\left(\frac{\partial u}{\partial x} + \nu\frac{\partial v}{\partial y}\right)\left(\frac{\partial w}{\partial x}\right)^2 + \left(\frac{\partial v}{\partial y} + \nu\frac{\partial u}{\partial x}\right)\left(\frac{\partial w}{\partial y}\right)^2 + (1-\nu)\left(\frac{\partial u}{\partial y} + \frac{\partial v}{\partial x}\right)\left(\frac{\partial w}{\partial x}\right)\left(\frac{\partial w}{\partial y}\right)\right\}dxdy \tag{7}$$

$$U_4 = \frac{3D}{2h^2}\iint\left\{\left(\frac{\partial w}{\partial x}\right)^2 + \left(\frac{\partial w}{\partial y}\right)^2\right\}^2 dxdy \tag{8}$$

where U_1 and U_2 are the quadratic-order strain energies representing the stretching and bending effects of the plate, respectively; the cubic-order strain energy U_3 represents the coupling of the bending and stretching effects; and the quartic-order strain energy U_4 represents the effect of the slope due to large deflections.

Triangular Plate Finite Element

The use of a quintic polynomial displacement function in the development of conforming triangular plate elements with small deflection by several independent investigators was reviewed by Zienkiewicz.[28] For a complete quintic polynomial displacement component, the 21 constants can be determined by the displacement and its first and second derivatives at each vertex of the triangle and the normal slopes at three midside nodes. By imposing three constraints the midside nodes can be eliminated and the variation of normal slope along an edge becomes a cubic polynomial. The 18 constant displacement field is thus obtained.

Since the large deflection problem of plates involves the coupling of inplane and out-of-plane effects, the element should be capable of representing both types of behavior. In this study, the linear formulation of a 54 d.o.f. triangular shell element[26] is extended to include the geometrically nonlinear terms for plate analysis. The element is shown in Fig. 1. The axes x, y, z and ξ, η, ζ are the global and local coordinates, respectively. The x-y and ξ-η planes coincide with the middle plane of the element. Each of the three displacement functions is assumed as a polynomial to the complete fifth order of ξ and η minus the term $\xi^4\eta$,

$$u = \sum_{i=1}^{20}\alpha_i\xi^{m_i}\eta^{n_i} \quad v = \sum_{i=1}^{20}\beta_i\xi^{m_i}\eta^{n_i} \quad w = \sum_{i=1}^{20}\gamma_i\xi^{m_i}\eta^{n_i} \tag{9}$$

The term $\xi^4\eta$ in Eq. (9) is omitted to ensure that the slope normal to the edge $\eta = 0$ is in the form of a cubic polynomial. Two further constraints are imposed to ensure that the slopes normal to the remaining two edges of the element are also in the form of cubic polynomials. The number of independent coefficients is thus reduced to 18 per displacement component. The matrix which relates the 20 unspecified coefficients γ_i to the 18 nodal quantities for w displacement in local coordinates is denoted by $[T_2]$ (Ref. 21), which can now be used for the u and v displacements as well.

By substituting the displacement functions of Eq. (9) into Eqs. (5-8) and integrating over the plate area, the strain energy of an element in terms of the global coordinate system is obtained as

$$U_e = \frac{1}{2}\underset{1\times 54}{\{q\}^T}\ \underset{54\times 54}{[R]^T}\ \underset{54\times 60}{[T]^T}\left[\underset{60\times 60}{[k]} + \frac{1}{3}\underset{60\times 60}{[n_1]} + \frac{1}{6}\underset{60\times 60}{[n_2]}\right]\underset{60\times 54}{[T]}\ \underset{54\times 54}{[R]}\ \underset{54\times 1}{\{q\}} \tag{10}$$

Equation (10) is comprised of three terms which correspond to $U_1 + U_2$, U_3, and U_4, respectively, in Eqs. (5-8). The matrices $[k]$, $[n_1]$, and $[n_2]$ are of zero, first, and second order of $\{q\}$, respectively. The matrix $[R]$ transforms all the matrices from the local coordinates to the global coordinates, which is given explicitly in Ref. 26; matrix $[T]$ contains three submatrices $[T_2]$ along the diagonal for the three displacement components. For convenience of the present derivations, $[R]$ has been rearranged in the sequence that all the terms related to u displacement appear first, then v, and, finally, w. The column vector of global degrees of freedom $\{q\}$ comprised of the quantities

$$\underset{54\times 1}{\{q\}^T} = \lfloor \{q_u\}^T \,:\, \{q_v\}^T \,:\, \{q_w\}^T \rfloor \tag{11}$$

with

$$\{q_u\}^T = \lfloor (u,\ u_x,\ u_y,\ u_{xx},\ u_{xy},\ u_{yy})_1,$$
$$(u,\ u_x,\ldots,u_{yy})_2,\ (u,\ u_x,\ldots,u_{yy})_3 \rfloor \tag{12}$$

where the subscripts *1, 2,* and *3* denote the vertex number and the vectors $\{q_v\}$ and $\{q_w\}$ can be expressed in the same form as that for $\{q_u\}$ by replacing u with v and w, respectively, in Eq. (12).

The linear and nonlinear stiffness matrix equations are obtained as

$$\underset{60\times 60}{[k]} = \begin{bmatrix} k_{\xi\xi} & k_{\xi\eta} & 0 \\ k_{\eta\xi} & k_{\eta\eta} & 0 \\ 0 & 0 & k_{\zeta\zeta} \end{bmatrix}$$

$$\underset{60\times 60}{[n_1]} = \begin{bmatrix} 0 & 0 & \eta_{1_{\xi\zeta}} \\ 0 & 0 & \eta_{1_{\eta\zeta}} \\ \eta_{1_{\zeta\xi}} & \eta_{1_{\zeta\eta}} & \eta_{1_{\zeta\zeta}} \end{bmatrix}$$

$$\underset{60\times 60}{[n_2]} = \begin{bmatrix} 0 & 0 & 0 \\ 0 & 0 & 0 \\ 0 & 0 & \eta_{2_{\zeta\zeta}} \end{bmatrix} \tag{13}$$

The coefficients in each 20×20 submatrix are given as

$$(k_{\xi\xi})_{ij} = \frac{\partial^2 U_1}{\partial\alpha_i\partial\alpha_j};\quad (k_{\xi\eta})_{ij} = (k_{\eta\xi})_{ji} = \frac{\partial^2 U_1}{\partial\alpha_i\partial\beta_j}$$

$$(k_{\eta\eta})_{ij} = \frac{\partial^2 U_1}{\partial\beta_i\partial\beta_j};\quad (k_{\zeta\zeta})_{ij} = \frac{\partial^2 U_2}{\partial\gamma_i\partial\gamma_j}$$

$$(n_{1_{\xi\zeta}})_{ij} = (n_{1_{\zeta\xi}})_{ji} = \frac{\partial^2 U_3}{\partial\alpha_i\partial\gamma_j};\quad (n_{1_{\eta\zeta}})_{ij} = (n_{1_{\zeta\eta}})_{ji} = \frac{\partial^2 U_3}{\partial\beta_i\partial\gamma_j}$$

$$(n_{1_{\zeta\zeta}})_{ij} = \frac{\partial^2 U_3}{\partial\gamma_i\partial\gamma_j};\quad \text{and}\quad (n_{2_{\zeta\zeta}})_{ij} = \frac{\partial^2 U_4}{\partial\gamma_i\partial\gamma_j} \tag{14}$$

The linear stiffness matrix $[k]$ was derived in Ref. 26. The first- and the second-order incremental stiffness matrices, $[n_1]$ and $[n_2]$, are derived here.

Derivation of all the matrix coefficients involves a basic integral over the triangular area

$$\int\int \xi^m \eta^n \mathrm{d}\xi\mathrm{d}\eta = \phi(m,n) \tag{15}$$

where

$$\phi(m,n) = c^{n+1}\{a^{m+1} - (-b)^{m+1}\} m!n!/(m+n+2)! \tag{16}$$

and *a, b,* and *c* are element dimensions as shown in Fig. 1.

The closed form expressions for the coefficients in the submatrices in Eqs. (13) are obtained using Eqs. (14),

$$(k_{\xi\xi})_{ij} = \frac{6D}{h^2}\left\{m_i m_j \phi(m_{ij}-2,n_{ij}) + \frac{1-\nu}{2} n_i n_j \phi(m_{ij},n_{ij}-2)\right\} \tag{17}$$

$$(k_{\xi\eta})_{ij} = \frac{6D}{h^2}\left\{\left(\nu m_i n_j + \frac{1-\nu}{2} n_i m_j\right)\phi(m_{ij}-1,n_{ij}-1)\right\} \tag{18}$$

$$(k_{\eta\eta})_{ij} = \frac{6D}{h^2}\left\{n_i n_j \phi(m_{ij},n_{ij}-2) + \frac{1-\nu}{2} m_i m_j \phi(m_{ij}-2,n_{ij})\right\} \tag{19}$$

$$\begin{aligned}(k_{\zeta\zeta})_{ij} = D\{&m_i m_j (m_i-1)(m_j-1)\phi(m_{ij}-4,n_{ij}) \\ &+ n_i n_j (n_i-1)(n_j-1)\phi(m_{ij},n_{ij}-4) \\ &+ [2(1-\nu) m_i m_j n_i n_j + \nu m_i n_j (m_i-1)(n_j-1) \\ &+ \nu m_j n_i (m_j-1)(n_i-1)]\phi(m_{ij}-2,n_{ij}-2)\}\end{aligned} \tag{20}$$

$$\begin{aligned}(n_{1_{\xi\zeta}})_{ij} = \frac{6D}{h^2}\sum_{k=1}^{20}\gamma_k\{&2m_i m_j m_k \phi(m_{ijk}-3,n_{ijk}) \\ &+ [2\nu m_i n_j n_k + (1-\nu)(n_i m_j n_k + n_i n_j m_k)] \\ &\times \phi(m_{ijk}-1,n_{ijk}-2)\}\end{aligned} \tag{21}$$

$$\begin{aligned}(n_{1_{\eta\zeta}})_{ij} = \frac{6D}{h^2}\sum_{k=1}^{20}\gamma_k\{&[2\nu n_i m_j m_k + (1-\nu)(m_i n_j m_k \\ &+ m_i m_j n_k)]\phi(m_{ijk}-2,n_{ijk}-1) \\ &+ 2n_i n_j n_k \phi(m_{ijk},n_{ijk}-3)\}\end{aligned} \tag{22}$$

$$\begin{aligned}(n_{1_{\zeta\zeta}})_{ij} = \frac{6D}{h^2}\Bigg\{&\sum_{k=1}^{20}\alpha_k[2m_i m_j m_k \phi(m_{ijk}-3,n_{ijk}) \\ &+ 2\nu n_i n_j m_k \phi(m_{ijk}-1,n_{ijk}-2) \\ &+ (1-\nu)(n_i m_j n_k + m_i n_j n_k)\phi(m_{ijk}-1,n_{ijk}-2)] \\ &+ \sum_{k=1}^{20}\beta_k[2n_i n_j n_k \phi(m_{ijk},n_{ijk}-3) \\ &+ 2\nu m_i m_j n_k \phi(m_{ijk}-2,n_{ijk}-1) \\ &+ (1-\nu)(n_i m_j m_k + m_i n_j m_k)\phi(m_{ijk}-2,n_{ijk}-1)]\Bigg\}\end{aligned} \tag{23}$$

$$\begin{aligned}(n_{2_{\zeta\zeta}})_{ij} = \frac{6D}{h^2}\sum_{k=1}^{20}\sum_{\ell=1}^{20}\gamma_k\gamma_\ell\{&3m_i m_j m_k m_\ell \phi(m_{ijk\ell}-4,n_{ijk\ell}) \\ &+ 3n_i n_j n_k n_\ell \phi(m_{ijk\ell},n_{ijk\ell}-4) \\ &+ [(m_i m_j n_k n_\ell + n_i n_j m_k m_\ell) + m_i n_j (m_k n_\ell + m_\ell n_k) \\ &+ n_i m_j (m_k n_\ell + n_k m_\ell)]\phi(m_{ijk\ell}-2,n_{ijk\ell}-2)\}\end{aligned} \tag{24}$$

where i and j vary from 1 to 20 and with

$$m_{ij} = m_i + m_j;\ m_{ijk} = m_i + m_j + m_k;\ m_{ijk\ell} = m_i + m_j + m_k + m_\ell;$$
$$n_{ij} = n_i + n_j;\ n_{ijk} = n_i + n_j + n_k;\ n_{ijk\ell} = n_i + n_j + n_k + n_\ell$$

Due to the high order of displacement functions and high number of degrees of freedom used in this element, the work equivalent consistent loads are used.

The kinetic energy of an element is given as

$$T_e = \tfrac{1}{2}\{\dot{q}\}^T [m]\{\dot{q}\} \tag{25}$$

The so-called consistent mass matrix $[m]$ relative to the global coordinates is obtained as

$$\underset{54\times 54}{[m]} = \begin{bmatrix} 0 & 0 & 0 \\ 0 & 0 & 0 \\ 0 & 0 & m_{ww} \end{bmatrix} \tag{26}$$

and

$$[m_{ww}] = [R_2]^T[T_2]^T[m_{\xi\xi}]\ [T_2]\ [R_2] \qquad (27)$$
$$18\times18 \quad 18\times18\ 18\times20\ 20\times20\ 20\times18\ 18\times18$$

where matrix $[R_2]$ transforms the matrix from local to global coordinates.[21] The coefficients in matrix $[m_{\xi\xi}]$ are given as

$$(m_{\xi\xi})_{ij} = \rho h \phi(m_{ij}, n_{ij}) \qquad (28)$$

where ρh is the mass density per unit area of the plate.

It is noted that the effects of inplane inertia are ignored in Eq. (26). Hence, the present formulation is valid for low-frequency modes.

Following the Lagrange's equation, the equation of motion for the present element is obtained as

$$\{p\} = [m]\{\ddot{q}\} + [[k] + \tfrac{1}{2}[n_1] + \tfrac{1}{3}[n_2]]\{q\} \qquad (29)$$

where $\{p\}$ is the consistent load vector.

Solution Procedures

By assembling the finite elements and applying the kinematic boundary conditions, the nonlinear equations of motion may be written as

$$\{P\} = [M]\{\ddot{Q}\} + [[K] + \tfrac{1}{2}[N_1] + \tfrac{1}{3}[N_2]]\{Q\} \qquad (30)$$

For a static problem, the direct solution of Eq. (30) can be done by numerical iteration. A powerful method of this type is the Newton-Raphson method,[28] which may be expressed symbolically as

$$[[K] + [N_1] + [N_2]]_i\{\Delta Q\}_{i+1} = \{\Delta P\}_i \qquad (31)$$

in which

$$\{\Delta P\}_i = \{P\} - [[K] + \tfrac{1}{2}[N_1] + \tfrac{1}{3}[N_2]]_i\{Q\}_i \qquad (32)$$

where Δ is an incremental operator. By solving Eq. (31), the improved displacement vector is found as

$$\{Q\}_{i+1} = \{Q\}_i + \{\Delta Q\}_{i+1} \qquad (33)$$

Subscript i denotes the iteration cycle.

In this study, the following maximum norm[29] is used for each cycle,

$$\|\epsilon\| = \max_i |\Delta Q_i / Q_{i,\text{ref}}| \le 10^{-3} \qquad (34)$$

For the analysis of linear vibration of plates about a buckled state, the eigenvalue equations based on Eq. (30) can be used, in which the incremental stiffness matrices $[N_1]$ and $[N_2]$ are based on the postbuckled equilibrium state.

For low-frequency large amplitude vibration, the inertial forces in the middle plane may still be neglected. The equations of motion for the assembled set of finite elements may be partitioned as

$$\begin{bmatrix} 0 & 0 \\ 0 & M \end{bmatrix}\begin{Bmatrix} \ddot{Q}_m \\ \ddot{Q}_f \end{Bmatrix} + \left[\begin{bmatrix} K_{mm} & 0 \\ 0 & K_{ff} \end{bmatrix} + \tfrac{1}{2}\begin{bmatrix} 0 & N_{1_{mf}} \\ N_{1_{fm}} & N_{1_{ff}} \end{bmatrix} + \tfrac{1}{3}\begin{bmatrix} 0 & 0 \\ 0 & N_{2_{ff}} \end{bmatrix} \right] \times \begin{Bmatrix} Q_m \\ Q_f \end{Bmatrix} = \begin{Bmatrix} P_m = 0 \\ P_f \end{Bmatrix} \qquad (35)$$

Let it be assumed that

$$\begin{Bmatrix} Q_m \\ Q_f \end{Bmatrix} = \begin{Bmatrix} \bar{Q}_m \psi(t) \\ \bar{Q}_f \tau(t) \end{Bmatrix} \qquad (36)$$

Multiplying out Eq. (35) and writing $\{Q_m\}$ in terms of $\{Q_f\}$ give

$$[M]\{\bar{Q}_f\}\ddot{\tau} + [K_{ff}]\{\bar{Q}_f\}\tau + [\bar{K}]\{\bar{Q}_f\}\tau^3 = \{P_f\} \qquad (37a)$$

where

$$[\bar{K}] = \tfrac{1}{2}[N_{1_{ff}}] + \tfrac{1}{3}[N_{2_{ff}}] - \tfrac{1}{4}[N_{1_{fm}}][K_{mm}]^{-1}[N_{1_{mf}}] \qquad (37b)$$

Assuming $\tau(t) = A\sin\omega t$ in Eq. (37a) and neglecting the third harmonic term $\sin 3\omega t$ give the eigenvalue equations for large amplitude free vibration of plates

$$[[K_{ff}] + \tfrac{3}{4}[\bar{K}] - \omega^2[M]]\{\bar{Q}_f\} = \{0\} \qquad (38)$$

To solve the nonlinear eigenvalue Eq. (38), an iterative procedure is used.[19,20] For a particular mode and given maximum amplitude, the iteration starts from an initial mode shape obtained for small amplitude vibration with amplitudes scaled up by a factor. Based on this initial mode shape, the nonlinear stiffness matrix $[\bar{K}]$ is formed and an eigenvalue and the corresponding eigenvector are found. The eigenvector is scaled up again and the iteration continues until the convergence criterion $\|\epsilon\|$ for frequency is achieved,

$$\|\epsilon\| = |\Delta\omega/\omega| \le 10^{-3} \qquad (39)$$

where $\Delta\omega$ is the change in frequency during the ith iterative cycle.

For large amplitude vibration of plates with inplane edge loading, the equations of motion Eq. (38) are modified as[22,30]

$$[[K_{ff}] + [K_\sigma] + \tfrac{3}{4}[\bar{K}] - \omega^2[M]]\{\bar{Q}_f\} = \{0\} \qquad (40)$$

where $[K_\sigma]$ is the assembled initial stress matrix.[31] This equation is solved by the same iterative scheme as described for Eq. (38).

Results

In order to ensure that the present geometrically nonlinear formulations and solution procedures are efficient and accurate when applied to the plate problems such as large deflection, postbuckling, small amplitude vibration about a buckled state, and large amplitude vibration with and without initial inplane stresses, a series of examples was selected and the results were compared with alternative solutions. A key development is that the two inplane displacement functions are assumed to be of the same order as the transverse deflection function in order to account for the coupling effect between the membrane and flexural behaviors and to treat the inplane boundary conditions more accurately and efficiently.

The linear formulation for the bending behavior of the present element was evaluated.[21] A first logical step is to evaluate the inplane behavior of the present finite element by considering a plane stress problem.

Parabolically Loaded Plane Stress Problem

A square plate loaded on two opposite sides by a parabolically distributed normal stress was studied. A quadrant was analyzed due to symmetry. This problem was solved by Cowper et al.[27] using a triangular element which contains a cubic polynomial with 10 constants in each of the two inplane displacement functions. The results for displacements and stresses at selected locations and the total strain energy obtained from both Ref. 27 and this study were plotted as relative error vs number of degrees of freedom in

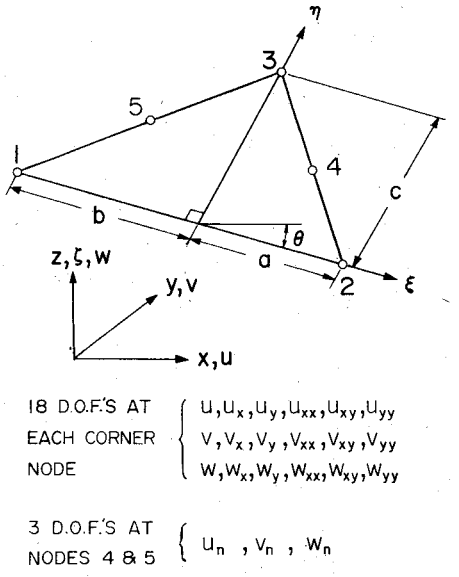

Fig. 1 Local and global coordinate systems of a 54 d.o.f. triangular plate element (reduced from 60 to 54 d.o.f.'s).

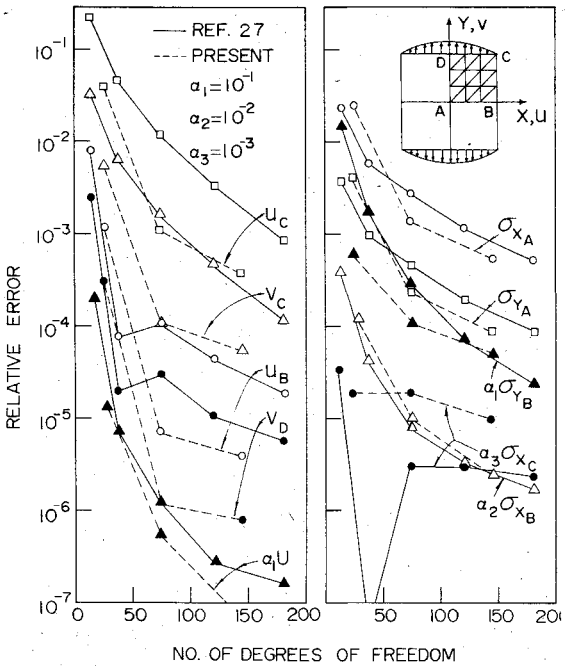

Fig. 2 Relative error for parabolically loaded plane stress problem, $\nu = 0.3$.

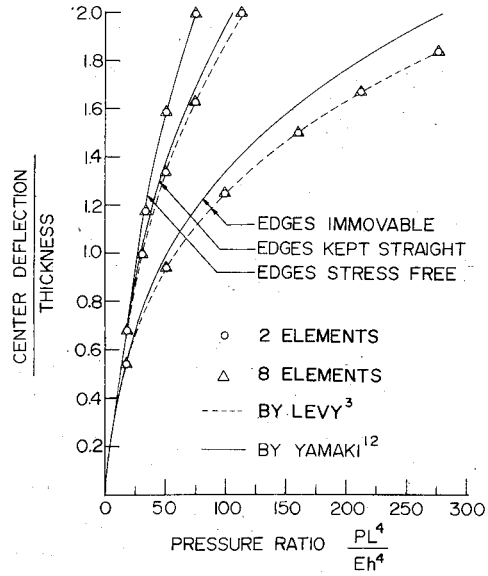

Fig. 3 Load-deflection curves for the simply supported square plate, $\nu = 0.316$.

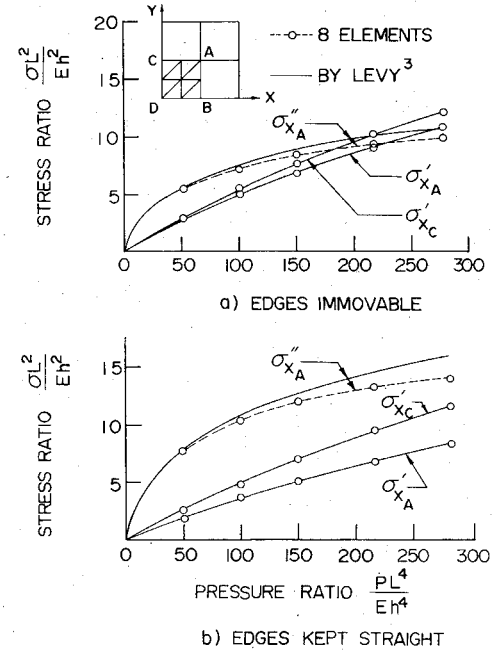

Fig. 4 Load vs membrane stresses (σ') and bending stresses (σ'') for the simply supported square plate, $\nu = 0.316$.

Fig. 2 for comparison. It is seen that the membrane portion of this element behaves accurately and efficiently and appears suitable for use in analyzing the geometrically nonlinear problems of plates.

Large Deflection of Square Plate under Uniform Lateral Loads

A simply supported square plate with length L, thickness h, and modulus of elasticity E under a uniform lateral pressure P was analyzed. Three inplane edge conditions were considered: 1) all edges immovable, 2) all edges kept straight, and 3) all edges stress free. Due to symmetry, only a quadrant need be analyzed and 1×1 and 2×2 meshes were used. The results for nondimensional center deflection vs pressure were plotted in Fig. 3. For each load increment, the Newton-Raphson iteration method was used.

This problem was analyzed, among others, by Levy[3,4] using a six-term trigonometric series representing the deflection and by Yamaki[12] using Galerkin's method with one-term approximation. Both sets of results were also plotted in Fig. 3 for comparison. The present results are in excellent agreement with those by Levy for boundary conditions 1 and 2 and also in excellent agreement with those by Yamaki for boundary condition 3. The results for the membrane and extreme fiber bending stresses at selected points for boundary conditions 1 and 2 were also plotted in Fig. 4. The membrane stresses agree well with those by Levy. The bending stresses, however, are 10% lower than those obtained by Levy at the higher load level.

A clamped square plate was next examined. The load-deflection curves were shown in Fig. 5. For boundary condition 1, the present results exhibit very small discrepancies as compared to Levy's. When comparing the present results with those by Yamaki, however, the trend of the curves are the same but small discrepancies are observed for all three boundary conditions. The results for the membrane (σ') and extreme-fiber bending stresses (σ'') at the center and midedge of the plate were given in Fig. 6. The present results are in

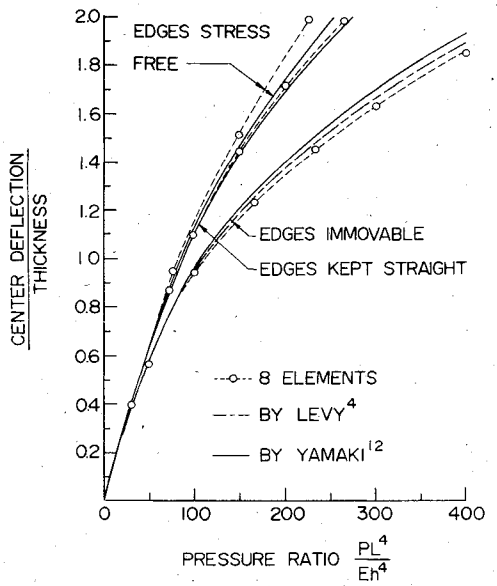

Fig. 5 Load-deflection curves for the clamped square plate, $\nu = 0.316$.

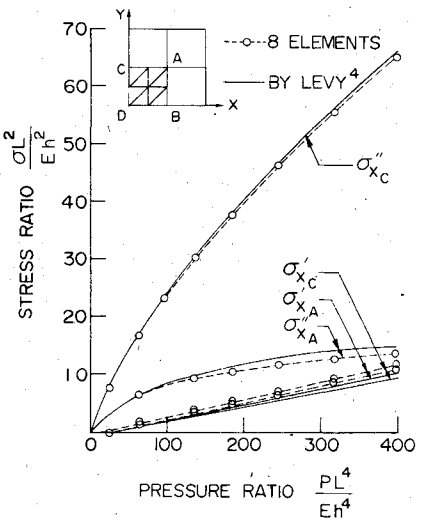

Fig. 6 Load vs membrane stresses (σ') and bending stresses (σ'') for the clamped square plate, $\nu = 0.316$.

good agreement with those by Levy.[4]

For both simply supported and clamped plates, no results for stresses are available from Ref. 12 for comparison.

Postbuckling of a Simply Supported Square Plate Subjected to Uniaxial Compression

A simply supported square plate with two sets of inplane boundary conditions were considered. In both cases the loaded edges of the plate were maintained straight with zero shear stress. In case 1, the unloaded edges were kept straight by a distribution of normal membrane stress, the resultant of which was zero. In case 2, the unloaded edges were free from stresses and free to wave in the plane of the plate. A 2×2 finite element mesh was used to idealize a quadrant of the plate. The Euler buckling load and the corresponding mode shape were found first, this mode shape was then scaled up by an initial deflection factor in order to form the nonlinear stiffness matrix. The Newton-Raphson iteration method was used at each load increment. The results for center deflection vs inplane compression for both cases were shown in Fig. 7 and compared with alternative solutions from Refs. 3, 7, and 8, respectively. Excellent agreement is observed. The results for membrane and extreme-fiber bending stresses were also compared with those by Levy in Figs. 8 and 9, respectively.

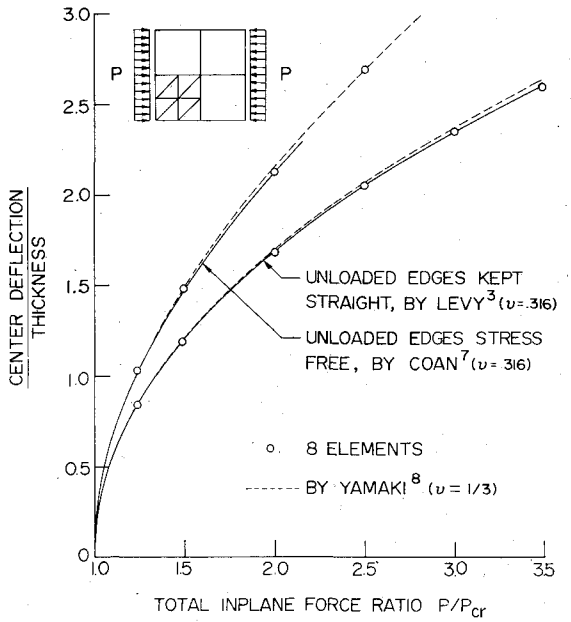

Fig. 7 Postbuckling load-deflection curve for the simply supported square plate.

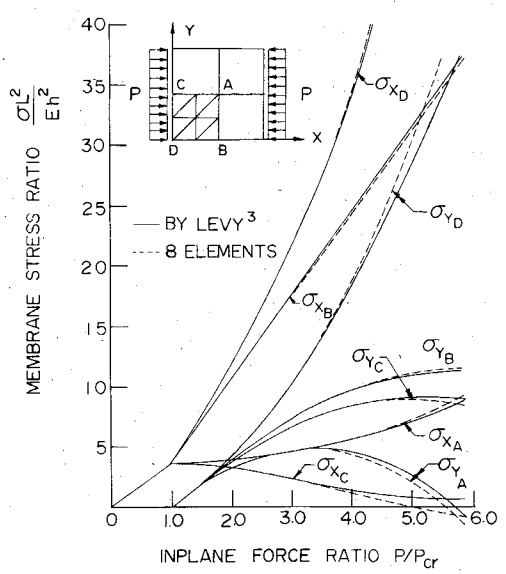

Fig. 8 Postbuckling membrane stresses of simply supported square plate with all edges kept straight, $\nu = 0.316$.

The agreement in membrane stresses is excellent. The strong performance of this element in predicting the membrane behavior is evident.

Small Amplitude Free Vibration of Buckled Plate

Although the problem of small amplitude free vibration of buckled plate has significant application to the design and analysis of aeronautical and space panel components, the work done in this area is relatively scarce. Bisplinghoff and Pian[9] studied the vibration problem of a rectangular plate with aspect ratio of 3 to 1 buckled due to uniaxial inplane compression applied on two shorter edges, induced by temperature rise. The plate was assumed as simply supported. A uniform shortening was prescribed between the two shorter edges, while the two longer edges were assumed free to move in the middle plane as straight edges. They used a one-term double sinusoidal function to represent the postbuckling mode and used additional three-term double sinusoidal functions to represent the vibration mode. The frequencies for the three fundamental symmetrical modes were found by using Lagrange's equation. The results from Ref. 9 for

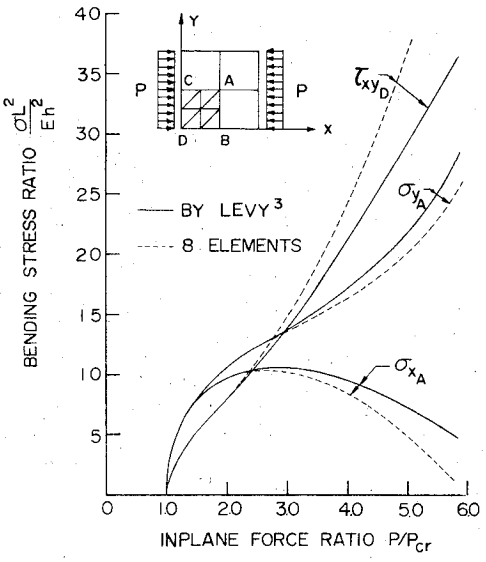

Fig. 9 Postbuckling bending stresses at locations A, B, C, and D of simply supported square plate with edges kept straight, $\nu = 0.316$.

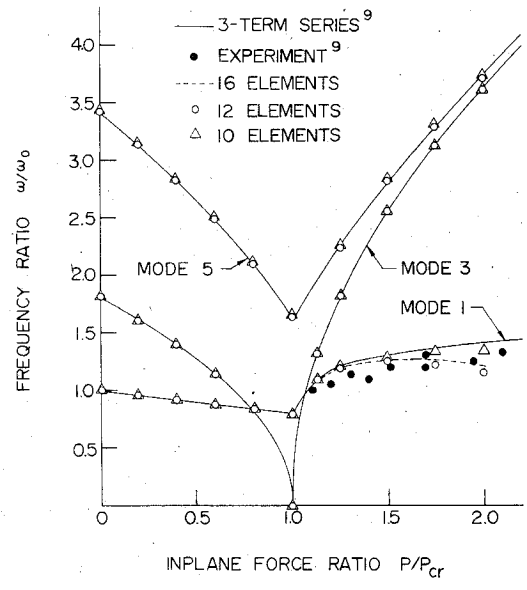

Fig. 10 Natural frequencies of the symmetrical modes for the buckled rectangular plates with aspect ratio of 3:1 ($\nu = 0.3$).

natural frequency ratio (ω/ω_0) vs inplane compression P due to temperature rise ΔT are shown in Fig. 10. In the buckled region, P and ΔT are related by

$$\frac{1}{2}\left(\frac{\Delta T}{\Delta T_{cr}} + 1\right) = \frac{P}{P_{cr}} \tag{41}$$

and ω_0 is the lowest linear natural frequency of the simply supported plate. The experimental data given in Ref. 9 were also plotted in Fig. 10. Because the aspect ratio is 3 to 1 for this simply supported plate, the lowest buckling mode contains three half sinusoidal waves, each being the same as that for a square plate. In the present analysis, it was indeed found that the load vs maximum deflection curve for the 3:1 plate is the same as that obtained in Fig. 7 for a square plate with all edges kept straight.

Due to symmetry about the longitudinal center line, a half of the plate was analyzed and three meshes with 10, 12, and 16 elements, respectively, were used. All the meshes were based on one layer of elements across half of the plate width. The present finite element solution yielded not only symmetrical modes but also antisymmetrical modes. When performing the free vibration analysis, all the loaded edges were assumed as fixed from inplane movement. The results for the lowest

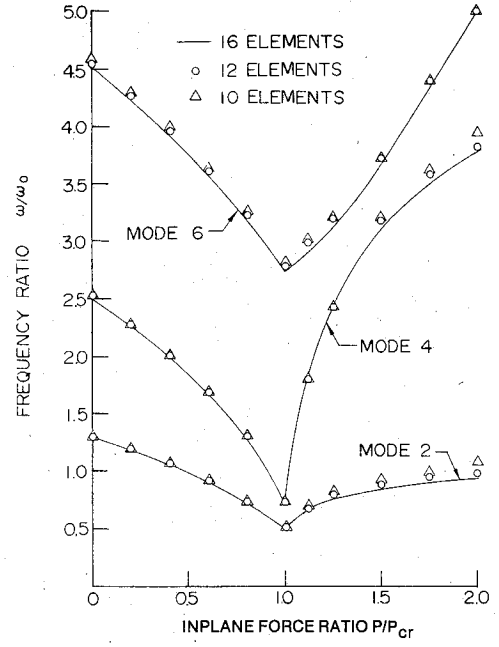

Fig. 11 Natural frequencies of the antisymmetrical modes for the buckled rectangular plate with aspect ratio of 3:1 ($\nu = 0.3$).

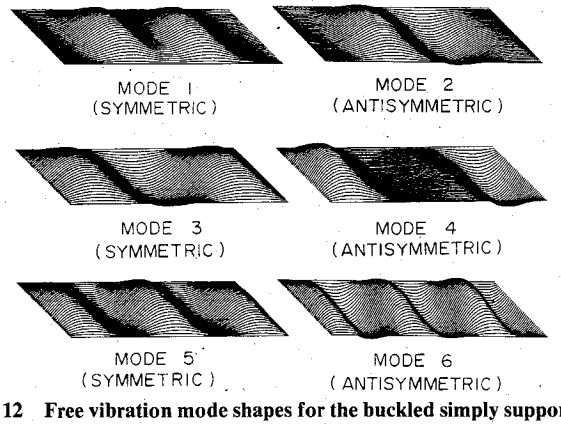

Fig. 12 Free vibration mode shapes for the buckled simply supported rectangular plate.

The mode shapes associated with each curve were plotted by Calcomp in Fig. 12. These modes were plotted on the basis of the dimensionless eigenvectors obtained from the free vibration analysis without superimposing them upon the postbuckled mode shape.

It is seen in Fig. 10 that the present results in natural frequency for modes 3 and 5 are in excellent agreement with the analytical solution of Ref. 9. The results for mode 1 exhibit some discrepancy from the analytical solution but agree well with the experimental data of Ref. 9. No alternative solutions are available for comparison with the results in Fig. 11.

Large Amplitude Free Flexural Vibration of Plates

A square plate with all edges either simply supported or clamped was studied. Three inplane boundary conditions were considered: 1) edges immovable, 2) edges kept straight, and 3) edges stress free.

Large amplitude vibration analyses were performed, among others,[10,11,13-15,18,19] by Yamaki[12] using a one-term Galerkin method and by Mei et al.[20] using the 18 d.o.f. triangular plate elements.[21] In Refs. 19 and 20, neither any degrees of freedom nor strains associated with the two inplane displacement components u and v were included in the finite element equations, thus the edges for all the plates considered were fixed from inplane movements.

The results for the first mode period vs center amplitude

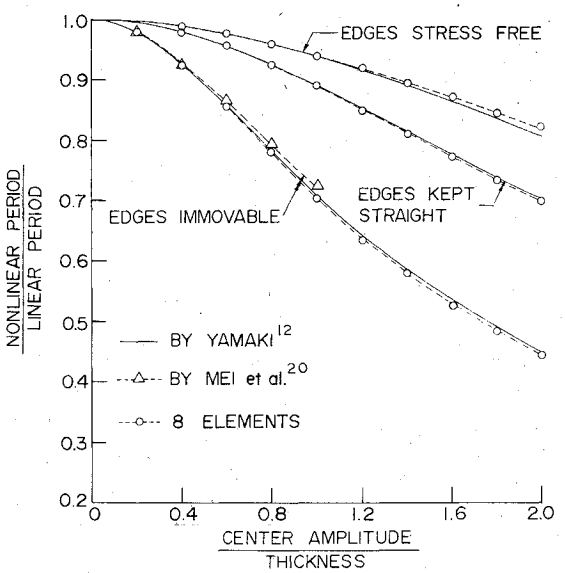

Fig. 13 First mode period of large amplitude vibration of simply supported square plates, $\nu = 0.3$.

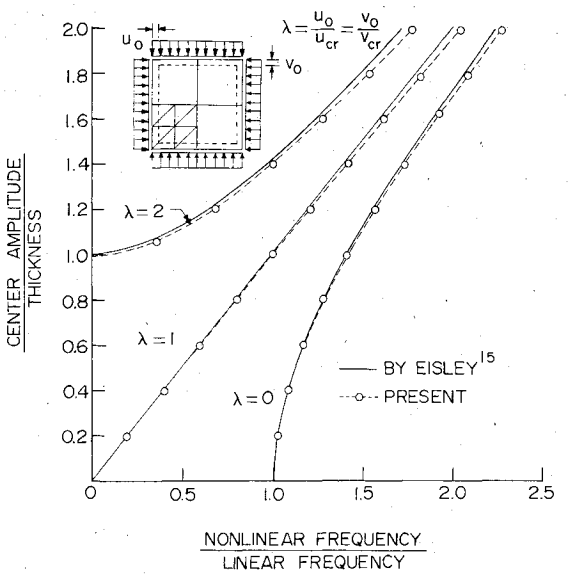

Fig. 15 First mode large amplitude vibrations of a simply supported square plate loaded in edges compression, $\nu = 0.3$.

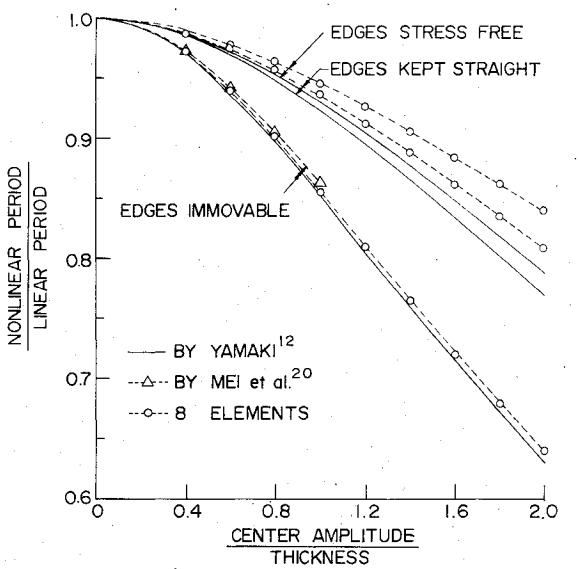

Fig. 14 First mode period of large amplitude vibration of clamped square plates, $\nu = 0.3$.

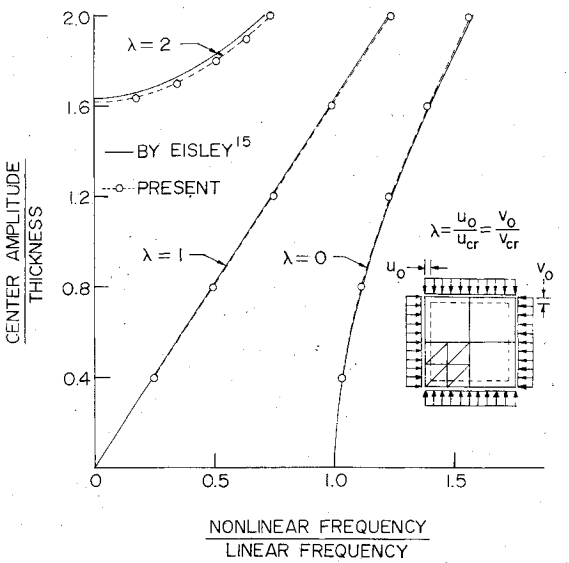

Fig. 16 First mode large amplitude vibration of a clamped square plate loaded in edges compression, $\nu = 0.3$.

supported square plate. A two-element model was also used and very slight differences were found between the eight- and the two-element solutions. The present results are in excellent agreement with those obtained by Yamaki[12] using the one-term Galerkin method.

In Refs. 19 and 20, the inplane deformations were neglected. This means that less strain energy was considered and, thus, longer periods might be predicted.

Results for clamped plates were shown in Fig. 14. For the inplane edge condition of immovable edges, the present eight-element results are in excellent agreement with those obtained by Yamaki[12] using the one-term Galerkin method. For the inplane edge conditions of stress free edges and straight edges, the present results for the nonlinear period are higher than the corresponding results by Yamaki[12] with the highest discrepancy being 5 ~ 7%.

Large Amplitude Vibration of Plates with Initial Stresses

A simply supported square plate under equal biaxial uniform edge compressive stress σ_0 was considered. The stress σ_0 produces two equal orthogonal uniform edge displacements u_0 and v_0. When σ_0 reaches its critical buckling value, the corresponding u_0 and v_0 are defined as u_{cr}. The effect of u_0/u_{cr} on the curves for nonlinear frequency vs center amplitude was investigated. Eight elements were used to model a quadrant. The results were shown in Fig. 15 for $u_0/u_{cr} = 0$, 1, and 2, respectively. This problem was studied by Eisley[15] using a one-term Galerkin method. His results were also shown in Fig. 15 for comparison. The agreement between the two solutions is excellent in all three cases.

For the case $u_0 = v_0 = 0$, both the present and Eisley's curves are identical to those obtained in this study and by Yamaki, respectively, as shown in Fig. 13, for the edge immovable case.

For the case $u_0/u_{cr} = 1$, σ_0 equals the Euler buckling stress σ_{cr}, the determinant of the sum of the linear stiffness matrix, and the initial stress matrix vanishes. As a result, the nonlinear free vibration eigenvalue equations are dominated by the mass matrix which contains ω^2 and the incremental stiffness matrices which contain quadratic terms of amplitudes. Thus, the amplitude-frequency curve appears to be nearly linear.

For $u_0/u_{cr} = 2$, the present solution and that of Eisley[15] are based on the assumption that the vibration of the plate is

symmetric about the flat position. Another type of motion is possible in which the plate vibrates about a static buckled position on one side of the flat position. Such motion is not considered here.

Similar results for a clamped square plate were plotted in Fig. 16. The trends for all the curves are quite similar to those shown in Fig. 15. The results obtained for all three λ values are in excellent agreement with those found by Eisley.[15]

Concluding Remarks

In the geometrically nonlinear problems of plates, the membrane and bending behaviors are coupled and the inplane edge conditions are as important as the flexural boundary conditions. Thus, it becomes necessary to model the inplane displacement components with a high degree of sophistication. In this development, the nonlinear stiffness matrices were formulated for a 54 degree of freedom triangular element for which each of the three orthogonal displacement components is represented by the same quintic polynomial in the plane coordinates x and y. The element has the capability to accurately account for the inplane deformations and inplane edge conditions. The Newton-Raphson iterative method was used. A variety of examples such as a parabolically loaded plane stress problem, large deflection and postbuckling of plates, free vibration of a buckled plate, and large amplitude vibrations of plates with and without inplane forces were investigated and comparisons were made with alternative solutions. Physical interpretations of the results were given. The versatility and accuracy of the present finite element development were demonstrated.

With such successful developments, research is now underway to study the geometrically nonlinear aeroelastic behaviors of panels in supersonic and transonic flows.

References

[1] Timoshenko, S. and Woinowsky-Kreiger, S., *Theory of Plates and Shells*, 2nd ed., McGraw-Hill Book Co., Inc., New York, 1959, pp. 396-428.

[2] Way, S., "Uniformly Loaded, Clamped, Rectangular Plates with Large Deflections," *Proceedings of the 5th International Congress for Applied Mechanics*, Cambridge, Mass., 1938, John Wiley & Sons, Inc., New York, 1939, pp. 123-128.

[3] Levy, S., "Bending of Rectangular Plates with Large Deflections," NACA TR-737, 1942.

[4] Levy, S., "Square Plate with Clamped Edges under Normal Pressure Producing Large Deflection," NACA TR-740, 1942.

[5] Wang, C. T., "Bending of Rectangular Plates with Large Deflections," NACA TN-1462, 1948.

[6] Berger, H. M., "A New Approach to the Analysis of Large Deflections of Plates," *Journal of Applied Mechanics*, Vol. 22, Dec. 1955, pp. 465-472.

[7] Coan, J. M., "Large Deflection Theory for Plates with Small Initial Curvature Loaded in Edge Compression," *Journal of Applied Mechanics*, Vol. 18, June 1951, pp. 143-151.

[8] Yamaki, N., "Postbuckling Behavior of Rectangular Plates with Small Initial Curvature Loaded in Edge Compression," *Journal of Applied Mechanics*, Vol. 26, Sept. 1959, pp. 407-414, (continued) Vol. 27, June 1960, p. 335-342.

[9] Bisplinghoff, R. L. and Pian, T.H.H., "On the Vibration of Thermally Buckled Bars and Plates," *Proceedings of the 9th International Congress for Applied Mechanics*, Vol. 7, 1957, pp. 307-318.

[10] Herrmann, G., "Influence of Large Amplitudes on Flexural Motions of Elastic Plates," NACA TN-3578, 1955.

[11] Chu, H.N. and Herrmann, G., "Influence of Large Amplitudes on Free Flexural Vibrations of Rectangular Elastic Plates," *Journal of Applied Mechanics*, Vol. 23, 1956, pp. 532-540.

[12] Yamaki, N., "Influence of Large Amplitude on Flexural Vibrations of Elastic Plates," *ZAMM*, Vol. 41, 1961, pp. 501-510.

[13] Wah, T., "Large Amplitude Flexural Vibrations of Rectangular Plates," *International Journal of Mechanical Science*, Vol. 5, 1963, pp. 425-438.

[14] Pandalai, K.A.V., "A General Conclusion Regarding the Large Amplitude Flexural Vibration of Beams and Plates," *Israel Journal of Technology*, Vol. 11, 1973, pp. 321-324.

[15] Eisley, J. G., "Nonlinear Vibrations of Beams and Rectangular Plates," *ZAMP*, Vol. 15, 1964, pp. 167-175.

[16] Yang, T. Y., "A Finite Element Procedure for Postbuckling Analysis of Initially Curved Plates," AIAA Paper 71-357, April 1971.

[17] McNamara, J. F. and Marcal, P. V., "Incremental Stiffness Method for Finite Element Analysis of the Nonlinear Dynamics Problem," International Symposium on Numerical and Computer Methods in Structural Mechanics, Urbana, Ill., Sept. 1971.

[18] Mei, C., "Finite Element Displacement Method for Large Amplitude Free Flexural Vibrations of Beams and Plates," *Computers and Structures*, Vol. 3, 1973, pp. 163-174.

[19] Rao, G. V., Raju, L. S., and Raju, K. K., "A Finite Element Formulation for Large Amplitude Flexural Vibrations of Thin Rectangular Plates," *Computers and Structures*, Vol. 6, June 1976, pp. 163-167.

[20] Mei, C., Narayanaswami, R., and Rao, G. V., "Large Amplitude Free Flexural Vibrations of Thin Plates of Arbitrary Shape," *Computers and Structures*, Vol. 10, Aug. 1979, pp. 675-681.

[21] Cowper, G. R., Kosko, E., Lindberg, G. M., and Olson, M. D., "Static and Dynamic Applications of a High-Precision Triangular Plate Bending Element," *AIAA Journal*, Vol. 7, Oct. 1969, pp. 1957-1965.

[22] Mei, C., "Large Amplitude Vibrations of Plates with Initial Stresses," *Journal of Sound and Vibration*, Vol. 60, Oct. 1978, pp. 461-464.

[23] Murray, D. W. and Wilson, E. L., "Finite Element Postbuckling Analysis of Thin Elastic Plates," *AIAA Journal*, Vol. 7, Oct. 1969, pp. 1915-1920.

[24] Tabarrok, B. and Dost, S., "Some Variational Formulations for Large Deformation Analysis of Plates," *Computer Methods in Applied Mechanics and Engineering*, Vol. 22, June 1980, pp. 279-288.

[25] Gass, N. and Tabarrok, B., "Large Deformation Analysis of Plates and Cylindrical Shells by a Mixed Finite Element Method," *International Journal for Numerical Methods in Engineering*, Vol. 10, July-Aug. 1976, pp. 731-746.

[26] Dawe, D. J., "High-Order Triangular Finite Element for Shell Analysis," *International Journal of Solids and Structures*, Vol. 11, Oct. 1975, pp. 1097-1110.

[27] Cowper, G. R., Lindberg, G. M., and Olson, M. D., "A Shallow Shell Finite Element of Triangular Shape," *International Journal of Solids and Structures*, Vol. 6, Aug. 1970, pp. 1133-1156.

[28] Zienkiewicz, O. C., *The Finite Element Method*, 3rd ed., McGraw-Hill Book Co., New York 1977, pp. 262-264 and 452-454.

[29] Bergan, P. G. and Clough, R. W., "Large Deflection Analysis of Plates and Shallow Shells Using the Finite Element Method," *International Journal for Numerical Methods in Engineering*, Vol. 5, March-April 1973, pp. 543-556.

[30] Mei, C. and Yang, T. Y., "Free Vibrations of Finite Element Plates Subjected to Complex Middle-Plane Force Systems," *Journal of Sound and Vibration*, Vol. 23, July 1972, pp. 145-156.

[31] Tabarrok, B., Fenton, R. G., and Elsaie, A. M., "Application of a Refined Plate Bending Element to Buckling Problems," *Computers and Structures*, Vol. 4, Dec. 1974, pp. 1313-1321.